DIRECT NUMERICAL SIMULATION OF BINARY MIXING LAYERS

Nicolas Lardjane
L.C.S.R./E.P.E.E. - C.N.R.S.
1c, avenue de la Recherche Scientifique
45071 Orléans cedex2, France
lardjane@cnrs-orleans.fr

Ivan Fedioun
L.M.E./E.P.E.E. - Université d'Orléans
8, rue Léonard de Vinci
45072 Orléans cedex2, France
Ivan.Fedioun@univ-orleans.fr

Iskender Gökalp
L.C.S.R./E.P.E.E. - C.N.R.S.
1c, avenue de la Recherche Scientifique
45071 Orléans cedex2, France
gokalp@cnrs-orleans.fr

ABSTRACT

Direct Numerical Simulations of compressible binary free shear layers with high density ratio (such as H_2/O_2) are performed using a physically/numerically optimized solver. Reduction of early acoustic waves is achieved through temporal self-similar initial conditions. Spatial distribution and temporal evolution of subgrid terms emerging from the L.E.S. formalism are produced by *a posteriori* filtering of the D.N.S. database.

INTRODUCTION

Turbulent mixing of heterogeneous fluids with large density ratio is of prime importance in many engineering applications ranging from chemical plants to supersonic aircraft propulsion. At the moment, most of the numerical work dealing with such systems has been performed in the framework of heated, mono-species, mixing layers (Sarkar and Pantano, 2000). Attempts to generalize classical k-ε turbulence models to variable density flows are under progress but some statistical results are still ill predicted (Aupoix et al., 2000). Thus, Large Eddy Simulation (L.E.S.) seems to be a promising tool to achieve accurate simulation of multi-species fluid flows at reasonable CPU cost in regard to Direct Numerical Simulation (D.N.S.). Nevertheless, Favre filtering of the initial set of equations (mass, momentum, energy, species, state) leads to the emergence of extra unknown moments compared to the mono-species case, such as $\widetilde{TY_\alpha} - \tilde{T}\tilde{Y}_\alpha$ (with T: temperature and Y_α: mass fraction of species α), difficult to model and often neglected (Calhoon and Menon, 1996).
The main goal of this study is to perform accurate D.N.S. of multi-species 3D mixing layers, leading to a database to be filtered *a posteriori* in order to exhibit subgrid terms. First, the D.N.S. procedure is described, with emphasis on initial conditions, transport coefficients formulation and numerical optimization. The exact L.E.S. equations resulting from mass-averaged filtering are then derived, leading to the whole set of subgrid terms. These unknown moments are then numerically evaluated and compared in the N_2/O_2 and H_2/O_2 cases for modeling perspectives.

D.N.S. PROCEDURE

Basic governing equations

Navier Stokes equations cast in non-conservation form, using Einstein's summation convention, are first recalled for a mixture:

$$\frac{\partial \rho}{\partial t} + \rho u_{i,i} + \rho_{,i} u_i = 0 \qquad (1)$$

$$\rho\left(\frac{\partial u_i}{\partial t}+u_{i,j}u_j\right)=-p_{,i}+\tau_{ij,j} \qquad (2)$$

$$\rho\left(\frac{\partial e}{\partial t}+e_{,j}u_j\right)=-pu_{j,j}-q_{j,j}+u_{i,j}\tau_{ij} \qquad (3)$$

$$\rho\left(\frac{\partial Y_\alpha}{\partial t}+Y_{\alpha,j}u_j\right)=-J_{\alpha j,j} \qquad (4)$$

If the mixture is newtonian and obeys Stoke's hypothesis, the viscous stresses read as usual:

$$\tau_{ij}=\mu\left(u_{i,j}+u_{j,i}-\frac{2}{3}u_{k,k}\delta_{ij}\right) \qquad (5)$$

Neglecting Dufour effect, the heat flux results from partial enthalpies fluxes and Fourier law:

$$q_j=\sum_\alpha h_\alpha J_{\alpha j}-\kappa T_{,j} \qquad (6)$$

Where partial enthalpies are given by:

$$h_\alpha=\Delta h^0_\alpha+\int_{T_0}^{T} C_{p\alpha}(\theta)d\theta \qquad (7)$$

The mass flux of species α, neglecting Soret effect, follows Fick's law:

$$J_{\alpha j}=-D_{\alpha m}Y_{\alpha,j} \qquad (8)$$

Supposing perfect gases, $de=\overline{C_v}(T,Y_\alpha)dT$ with $\overline{C_v}=\sum_\alpha Y_\alpha C_{v\alpha}$. The equation of state of the mixture is then:

$$p=\rho\mathcal{R}T\sum_\alpha\frac{Y_\alpha}{W_\alpha} \qquad (9)$$

with $\mathcal{R}$ the universal gas constant and W_α the molecular weight of species α.

Numerical implementation

Numerical diffusion, linked to the approximation of (1)–(4), is reduced by use of centered compact finite difference schemes (Lele, 1992) in association with a 3^{rd} order low storage Runge-Kutta scheme. Spatial derivatives are 6^{th} order with a 4^{th} order one-sided scheme at non homogeneous boundaries where N.S.C.B.C. type conditions (Baum et al., 1994) are applied.

Navier Stokes equations (1)–(4) are cast in - rather unconventional for compressible flow - convective form for primitive variables ρ, u, v, e, Y since it reduces numerical aliasing errors and leads to a simpler formulation of boundary conditions (Fedioun et al., 2000).

Num. Proc.	Gflops	// efficiency
1	5.1	1.00
2	10.1	1.00
3	14.9	0.99
6	29.4	0.95

Table 1: Performances and parallel efficiency of the solver.

The effect of physical aliasing errors is illustrated on figure 1 for a temporal plane mixing layer. It affects mainly the pairing core region where the spectral content of the solution nearly reaches the numerical cutoff.

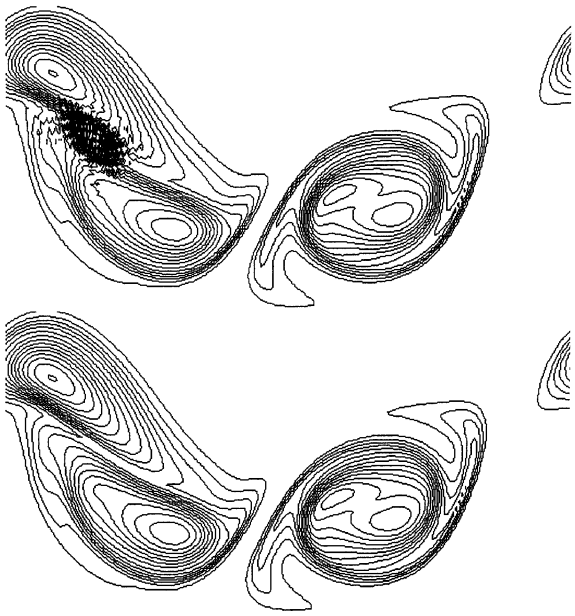

Figure 1: Vorticity field for divergence (top) and convective (bottom) forms.

So, a fully vectorized Fortran90 solver has been developed with explicit parallelism achieved through OpenMP. Sample performances on 1 to 6 NEC-SX5 processors are displayed in table 1.

Transport coefficients formulation

In equations (5) – (8), transport coefficients μ, κ and $D_{\alpha m}$ have to be prescribed for the mixture, in reference to pure species values. Wilke's and Wassiljewa's formulae (Reid et al., 1988) are suitable mixing laws for viscosity and thermal conductivity. If binary systems are considered, $D_{\alpha m}$ reduces to the binary diffusion coefficient $D_{12}=D_{21}$ of one species in the other, which may be accurately estimated as a function of temperature with Fuller's empirical correlation. Partial viscosities and thermal conductivities may be obtained from kinetic theory of gases, but Chung's empirical formulae are more accurate. Nevertheless, straightforward implementation of these formulae is prohibitively CPU time consuming. The in-

fluence of transport coefficients formulation on the statistics of the flow is analyzed by Lardjane et al. (2000). It is shown that constant coefficients give acceptable results in isothermal flows, even for the H_2/O_2 mixing layer at Re=100, at half a computational cost (fig. 2).

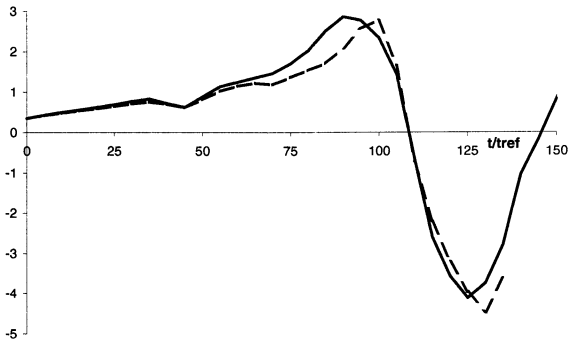

Figure 2: Compressible momentum thickness for variable (dashed) and constant (plain) transport coefficients formulation in the plane H_2/O_2 mixing layer.

Initial conditions

Temporal mixing layers are classically initialized with hyperbolic tangent velocity and mass fraction profiles. Nevertheless, considering Navier-Stokes equations as a mathematical operator, the response of this operator to the input signal is the generation of acoustic waves whose amplitudes are linked to the initial density ratio (fig. 3). For high density ratios, these waves may lead to numerical instabilities, despite of non reflecting boundary conditions. For the calculation to be feasible, a temporal alternative to the spatial Levy-Lees similarity solution (Kennedy and Gatsky, 1994) has been developed to match as close as possible an exact Navier-Stokes solution (Lardjane et al., 2001). The basic hypotheses of the temporal similarity approach are: unsteady flow, 2D 0^{th} order boundary layer approximation, $\partial/\partial x = 0$. It reduces the amplitude of early acoustic waves by two orders of magnitude in the H_2/O_2 case (fig. 3) with regards to the hyperbolic tangent approximation.

L.E.S. FORMALISM

In this section, sgs terms are produced from filtered Navier-Stokes equations. The associated discrete filtering procedure is presented.

Filtered equations

The Favre mass weighted filtering operator $\tilde{\phi} = \overline{\rho\phi}/\bar{\rho}$ applied to Navier-Stokes equations

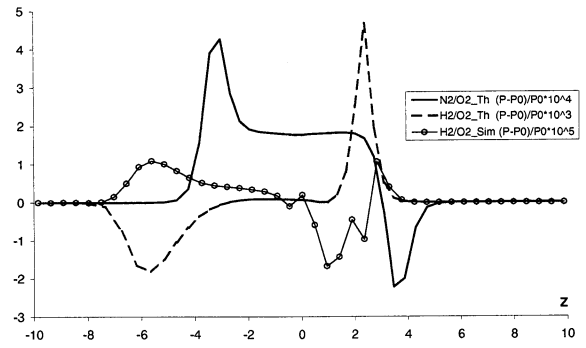

Figure 3: Transversal acoustic waves generated by an initial hyperbolic tangent field for $N_2 - O_2$ (plain), $H_2 - O_2$ (dashed), and a self-similar field for $H_2 - O_2$ (circle).

gives:

$$\frac{\partial \bar{\rho}}{\partial t} + (\bar{\rho}\tilde{u}_j)_{,j} = 0 \tag{10}$$

$$\frac{\partial(\bar{\rho}\tilde{u}_i)}{\partial t} + (\bar{\rho}\tilde{u}_i\tilde{u}_j)_{,j} = -\hat{p}_{,i} + \tau_{ij,j} + A_{i1} + A_{i2} + A_{i3} \tag{11}$$

$$\begin{aligned} \bar{\rho}\widetilde{C_v}\frac{\partial \tilde{T}}{\partial t} + \hat{p}\tilde{u}_{j,j} &= \left[\tilde{k}_{,j} - \sum_\alpha \widetilde{C_{p_\alpha}}\hat{J}_{\alpha j}\right]\tilde{T}_{,j} \\ &- \tilde{T}\sum_\alpha \widetilde{r}_\alpha\ \hat{J}_{\alpha j,j} + \tilde{k}\tilde{T}_{,jj} + \hat{\tau}_{ij}\tilde{u}_{i,j} \\ &+ B_1 + ... + B_{10} \end{aligned} \tag{12}$$

$$\frac{\partial\left(\bar{\rho}\tilde{Y}_\alpha\right)}{\partial t} + \left(\bar{\rho}\tilde{Y}_\alpha\tilde{u}_j\right)_{,j} = -\hat{J}_{\alpha j,j} + C_{\alpha 1} + C_{\alpha 2} \tag{13}$$

Using the following convention:

$$\bar{f}(\rho, u_i, T, Y_\alpha) = \hat{f}(\bar{\rho}, \tilde{u}_i, \tilde{T}, \tilde{Y}_\alpha) + \breve{f} \tag{14}$$

unknown moments formulate:

$$A_1 = -\left(\overline{\rho u_i u_j} - \bar{\rho}\tilde{u}_i\tilde{u}_j\right)_{,j} \tag{15}$$

$$A_2 = \breve{\tau}_{ij,j} \tag{16}$$

$$A_3 = -\breve{p}_{,j} \tag{17}$$

$$C_{\alpha 1} = -\left(\overline{\rho Y_\alpha u_j} - \bar{\rho}\tilde{Y}_\alpha\tilde{u}_j\right)_{,j} \tag{18}$$

$$C_{\alpha 2} = -\breve{J}_{\alpha j,j} \tag{19}$$

$$B_1 = -\tilde{T}_{,j} \sum_\alpha \widetilde{C_{p_\alpha}} \breve{J}_{\alpha j} \quad (20)$$

$$B_2 = -\tilde{T} \sum_\alpha \tilde{r}_\alpha \breve{J}_{\alpha j,j} \quad (21)$$

$$B_3 = \tilde{u}_{i,j} \breve{\tau}_{ij} \quad (22)$$

$$B_4 = \frac{\partial \breve{p}}{\partial t} + \tilde{u}_j \breve{p}_{,j} \quad (23)$$

$$B_5 = -\bar{\rho} \frac{\partial \breve{h}}{\partial t} + \tilde{u}_j \breve{h}_{,j} \quad (24)$$

$$B_6 = -\sum_\alpha \left[\left(\tilde{h}_\alpha - \tilde{r}_\alpha \tilde{T} \right) C_{\alpha 1} \right] \quad (25)$$

$$B_7 = -Q_{j,j} \quad (26)$$

$$B_8 = -\left(\overline{\rho e u_j} - \bar{\rho} \tilde{e} \tilde{u}_j \right)_{,j} \quad (27)$$

$$B_9 = -\left(\overline{p u_{j,j}} - \bar{p} \tilde{u}_{j,j} \right) \quad (28)$$

$$B_{10} = \overline{u_{i,j} \tau_{ij}} - \tilde{u}_{i,j} \bar{\tau}_{ij} \quad (29)$$

Discrete filtering

An explicit S.O.C.F. box filter (Ghosal and Moin, 1995) with adjustable width is used. In this approach, the physical coordinate x is linked to ξ in the computational domain by the bijective mapping function f.

$$\phi(x) = \phi\left(f^{-1}(\xi)\right) = \psi(\xi) \quad (30)$$

With $\bar{\Delta} = cste$ the cutoff length in the computational domain, any filtered variable reads:

$$\bar{\psi}(\xi) = \frac{1}{\bar{\Delta}} \int_\Omega \psi(\eta) G\left(\frac{\xi - \eta}{\bar{\Delta}} \right) d\eta \quad (31)$$

$$G(\theta) = \begin{cases} 1 & \text{if } \mid \theta \mid \leq \frac{1}{2} \\ 0 & \text{else} \end{cases} \quad (32)$$

It reduces, in homogeneous directions after a trapezoidal integration and $\bar{\Delta} = 2\alpha\Delta\xi$, to:

$$\bar{\phi}_i = \frac{1}{4\alpha} \left\{ \phi_{i-\alpha} + 2 \sum_{k=-\alpha+1}^{\alpha-1} \phi_{i+k} + \phi_{i+\alpha} \right\} \quad (33)$$

SUBGRID MOMENTS MAGNITUDE

D.N.S. calculations were performed on a NEC-SX5 supercomputer for the 3D temporal mixing layer between O_2 as the upper stream and either N_2 or H_2 as the lower one. Density ratios are respectively ≈ 1 and 16. Free stream velocities are $\pm 100 m/s$ with constant 300K temperature. The Reynolds number based on initial vorticity thickness is 100.

Box filtering is performed for $\alpha = 1, 2, 3$ in (33). Early tests have pointed out a linear trend in magnitude of sgs terms versus the filter width, so only results for $\alpha = 1$ are presented, averaged over periodic directions.

N_2O_2 case

This near unity density ratio test case allows comparison with previous mono-species simulations (Vreman, 1995). The non dimensional computational box is $L_x = 42$, $L_y = 42$, $L_z = \pm 40$ with clustering of grid points in the shear region, with spatial resolution $N_x = 181$, $N_y = 181$, $N_z = 245$, and a time step based on a 0.5 C.F.L. condition. The convective Mach number is 0.29.

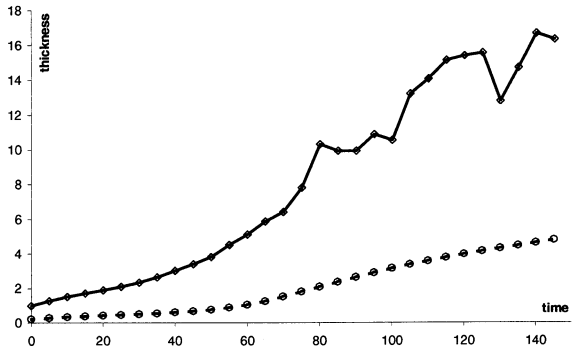

Figure 4: Evolution of vorticity thickness (solid) and momentum thickness (dashed) in the N_2/O_2 mixing layer.

The vorticity and momentum thicknesses are displayed in figure 4. Calculation was stopped at $t = 150$ before saturation of the box due to the temporal approach, which would have left a single roller. Three stages are distinguished in the time evolution of moments' extrema for the energy equation (12) (fig. 5). In the early stage of the simulation, viscous terms are predominant (e.g. B_{10}). Then, for $t \approx 10$ to 30, initial disturbances are linearly amplified by the dynamics leading to the emergence of B_8. A long non-linear stage follows, associated with pairing processes, filling up the energy spectrum. This last part leads to the re-predominance of the viscous term B_{10}. Basically, the most significant moments are B_6, B_8, B_9 and B_{10}, all involving velocity gradients.

Spatial repartition of moments (fig. 6), shows that B_6 and B_9 are nearly equivalent, and quasi opposite to B_8. It can be shown after some algebra that this behaviour is consistent with constant density and temperature assumptions provided the further condition $Y_{,j} << u_{i,j}$.

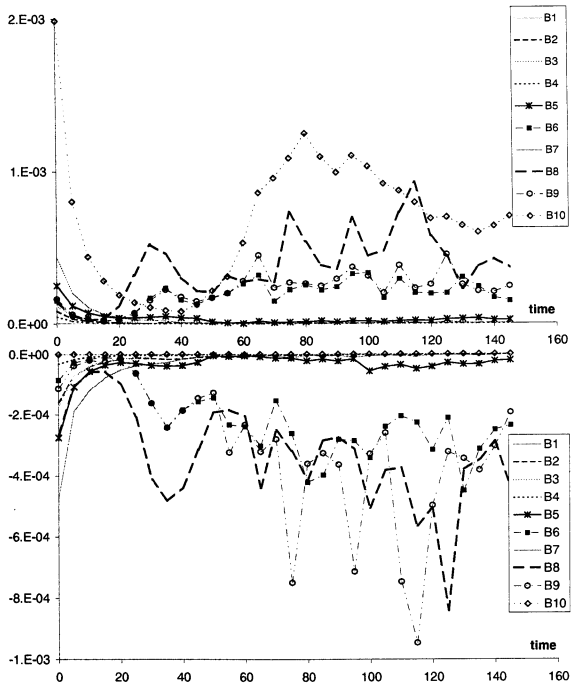

Figure 5: Time evolution of maximum (top) and minimum (bottom) of moments magnitude in the N_2/O_2 mixing layer.

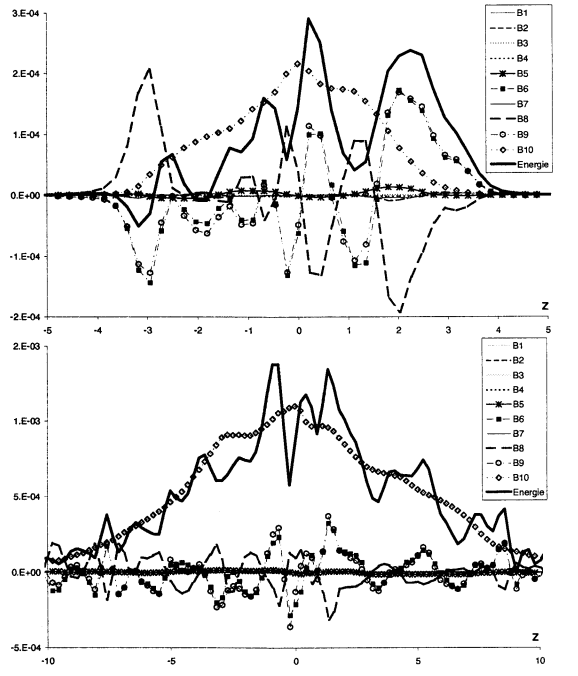

Figure 6: Moments magnitude in the N_2/O_2 mixing layer at t=50 (up) and t=95 (bottom).

This first test case leads to results similar to those of Vreman (1995) for mono-species simulation, mainly on the importance of B_{10}.

H_2O_2 case

Due to the stiffness of this case, increase in spatial resolution is needed: $L_x = 35$, $L_y = 35$, $L_z = -40/+20$, and $N_x = 199$, $N_y = 199$, $N_z = 486$. The C.F.L. condition of 0.9 limits drastically the time step. The convective Mach number is 0.12.

Time evolution of statistical features of the flow (fig. 7) show that the simulation was stopped (after 250h CPU time) before all pairing had occurred, so only early stages of the L.E.S. can be discussed.

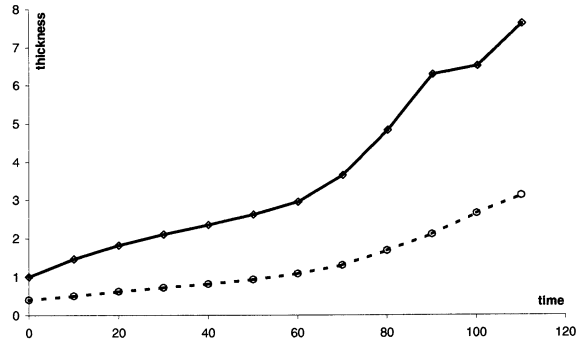

Figure 7: Evolution of vorticity thickness (solid) and momentum thickness (dashed) in the H_2/O_2 mixing layer.

The time evolution of moments' extrema (fig. 8) shows longer delays for the first two stages (comparatively to N_2/O_2), that is: the flow needs longer (non-dimensional) time to transfer the energy of initial perturbations towards fully developed turbulence. Here, two opposite phenomena (reduction of convective Mach number by a factor 2 and increase of density ratio by a factor 16) are in balance for the resulting growth rate of the shear layer (Brown and Roshko, 1974). At these low convective Mach numbers, density effects overcome compressibility ones.

Globally, the magnitude of subgrid terms is artificially higher than in the previous case, due to Favre's mass weighted averaging. From figure (9), there are still four leading terms: B_2, B_6, B_8, B_9. B_{10} is no more significant whereas B_2 (linked to species derivatives) becomes a key term for modeling issues. This term arises through different processes resulting from the large initial density ratio. These processes are at least the fact that $r_{H_2} >> r_{O_2}$, and that Favre weighting do not commute with derivatives.

CONCLUSION

This paper is a preliminary attempt to compare moments magnitude in L.E.S. of free shear flows with large density variations. Although it presents work in progress, some key features

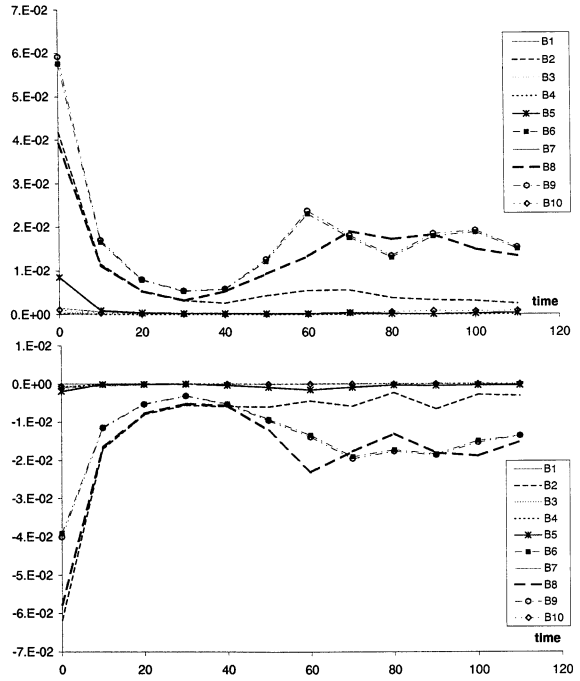

Figure 8: Time evolution of maximum (top) and minimum (bottom) of moments magnitude in the H_2/O_2 mixing layer.

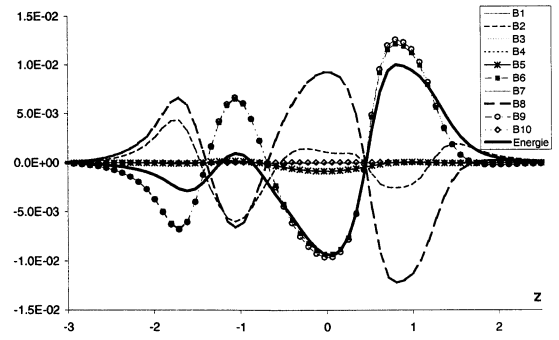

Figure 9: moments magnitude in the H_2/O_2 mixing layer at t=50.

have been pointed out.

The development of a high performance D.N.S. code has allowed the simulation of N_2/O_2 and H_2/O_2 3D mixing layers. Filtering of the N_2/O_2 database globally validated the method, for L.E.S. subgrid term evaluation, with mono-species results. The H_2/O_2 case showed emergence of a different balance in subgrid terms, at least in the early stages of the simulation. Further numerical experiments (longer time and higher Reynolds number) are necessary to validate definitely this first result. Non isothermal simulations should also be carried out since they could reveal importance of unsteady moments B_4 and B_5.

ACKNOWLEDGEMENT

Computational resources have been provided by CNRS at IDRIS - Institut de Développement et de Ressources en Informatique Scientifique in Orsay, France.

REFERENCES

Aupoix, B., Bezard, H., and Cartis, S., 2000, "Correction for density gradient effects in boundary and mixing layers", *Proceedings, Int. Conf. on Variable Density Turbulent Flows*, F. Anselmet et al., ed., Presses Universitaires de Perpignan, Banyuls, France, pp. 187-198.

Baum, M., Poinsot, T. J., Thévenin, D., 1994, "Accurate boundary conditions for multicomponent reactive flows", *Journal of Computational Physics*, Vol. 116, pp. 247-261.

Brown, G. L., Roshko, A., 1974, "On density effects and large structure in turbulent mixing layers", *Journal of Fluid Mechanics*, Vol. 64, pp. 775-816.

Calhoon, W., Menon, S., 1996, "Subgrid modelling for reacting large eddy simulation", *Proc. of the 34th Aerospace Sciences Meeting and Exhibit, AIAA*, Reno, Vol. 96-0516.

Fedioun, I., Lardjane, N., Gökalp, I., 2000, "Revisiting numerical errors in direct and large eddy simulations of turbulence: physical and spectral spaces analysis ", Submitted to *Journal of Computational Physics.*

Ghosal, S., Moin, P., 1995, "The basic equations for large-eddy simulation of turbulent flows in complex geometry", *Journal of Computational Physics*, Vol. 118, pp. 24-37.

Lardjane, N., Fedioun, I., Gökalp, I., 2000, "Formulation of transport coefficients in binary mixture of gases" *Proc., Int. Conf. on Variable Density Turbulent Flows*, France, pp. 87-98.

Lardjane, N., Fedioun, I., Gökalp, I., 2001, "Self-similar initial conditions for the direct numerical simulation of temporally growing high density ratio mixing layers", Submitted to *Journal of Fluid Mechanics*

Lele, S. K., 1992, "Compact finite difference schemes with spectral-like resolution", *Journal of Computational Physics*, Vol. 103, pp. 16-42.

Reid, R. C., Prausnitz, J. M., Poling, B. E., 1988, "The properties of gases and liquids - 4^{th} edition", Mac Graw Hill, Chem. Eng. Series.

Sarkar, S., Pantano, C., 2000, "Effects of density variation in compressible turbulent shear flows", *Proc., Int. Conf. on Variable Density Turbulent Flows*, France, pp. 109-127.

Vreman, A. W., 1995, "Direct and Large Eddy Simulation of the compressible turbulent Mixing Layer", Ph.D. Thesis, Dept. of Applied Mathematics, University of Twente.